# Optical Strain Detectors based on Gold/Elastomer Nanoparticulated Films

**Miguel A. Correa-Duarte,[1]* Verónica Salgueiriño-Maceira,[2] Antonio Rinaldi,[3] Karl Sieradzki,[3] Michael Giersig,[4] Luis M. Liz-Marzán[1]**

Departamento de Química Física and Unidad Asociada CSIC - Universidade de Vigo, 36310, Vigo, Spain
Departamento de Química Física, Universidade de Santiago de Compostela, 15782 Santiago de Compostela, Spain
School of Materials, Arizona State University, Tempe (AZ) USA, CAESAR, Ludwig-Edhard-Allee 2, 53175, Bonn, Germany

## Abstract

**The application of two different optical effects is demonstrated for the detection of strain applied to elastomeric films. On one hand, dense coatings made of silica-coated gold nanoparticles (Au@$SiO_2$ NPs), which are built up onto poly(dimethylsiloxane) (PDMS) elastomeric films, using the layer-by-layer (LbL) method, provide intense surface plasmon resonance (SPR) absorption. On the other hand, polystyrene spheres can be deposited as ordered monolayers to create patterned PDMS films with well-defined light diffraction. Both effects were used to monitor the structural damage of such PDMS films upon stretching, remaining both physical phenomena (absorption from the gold film and diffraction from the ordered structure) active for optical sensing applications in the early detection of structural damage in critical infrastructures.**

## Introduction

The assembly of nanocrystals into macroscopic thin films offers an exciting pathway for the construction of materials with specifically designed optical, electrical, and/or catalytic properties. Inasmuch as these materials, fabricated in the nanosize regime, are purported to possess advantageous properties, they provide new avenues for performance and functional gains in structures made with such nanomaterials which would be unthought of using conventional ones. In particular, nanoparticulated metallic films have been the focus of intense research, primarily due to the interest in their optical and electronic properties,[1] and thereby offering a high potential for the development of novel electrical and optical sensors and catalysts. In fact, there is a growing need to enhance the function of these engineered structures beyond their present boundaries through the use of advanced materials. Therefore, gold nanoparticles (NPs) with diameters ranging from 10nm to 100nm, with unique optical and electronic properties,[1-2] are attractive candidates for the construction of inorganic-organic hybrid structures, which can be applied in advanced spectroscopy, chemical and biosensor technology and microelectronic devices.[3-9]

One of the most attractive features of gold NPs is the observation of intense surface plasmon resonances (SPR), which lead to strong surface enhanced Raman scattering, as well as nonlinear optical properties. SPR arise from the coupling of conduction electrons with incident electromagnetic waves[10, 11] and are especially relevant in noble metals such as gold and silver, since the resonances occur within the visible range, though the precise frequency depends on various scattering conditions at the NPs interface.[12-14] For example, surface-enhanced Raman scattering (SERS) is a highly sensitive spectroscopic tool that can detect individual molecules adsorbed on silver or gold NPs.[11] The SERS effect mainly arises from the enhancement of the local electromagnetic field in the vicinity of the metal surface, which is strongly coupled to the excitation of the surface plasmon.[15]

In the case of nanoparticulated metallic films, their functional properties are also governed by the size,[16,17] shape,[18] and size distribution[19-21] of the metal NPs, in addition to the dielectric properties of the surrounding medium.[22] Therefore, various techniques have been developed in recent years for the construction of metallic nanoparticulated films on flat surfaces. Strategies for the immobilization of Au NP layers onto surfaces include either physical deposition (e.g., spin-coating[23] and spraying[24]) or layer-by-layer (LbL) schemes. Some LbL approaches that have been demonstrated include covalent schemes, primarily through surface attachment of NPs via dithiol linkages[25, 26] or mercaptosilanes,[27] and offer a better control over the film thickness and density. Electrostatic binding has also been demonstrated, including the use of charged molecules for attaching NPs to the surface[28-30], as well as polyelectrolyte systems.[28, 31-34] Gold NPs are usually preferred in these nanoparticulated films, because of their chemical stability and relatively simple preparation.

In fact, the reactivity of sulphur-containing molecules (thiols, disulfides, etc) toward Au surfaces, enabling formation of a large variety of self-assembled monolayers, can be exploited for chemical manipulation of Au surfaces.

It has also been of particular interest the formation of thin films with a high density of these metal NPs, which is often desired for catalytic and electronic applications. Thin films comprising a dense packing of gold NPs can be prepared by means of the adsorption of 4-(dimethylamino)pyridine gold NPs (DMAP-AuNP) onto preformed polyelectrolyte (PE) films.[35] The formation of these dense nanoparticulated films was attributed to the reversible binding nature of the DMAP ligand and the nature of the PE films (poly-(sodium 4-styrenesulfonate) (PSS) and poly(allylamine hydrochloride) (PAH)), which act as matrices for nanoparticle adsorption.[34-40] PAH/PSS multilayer films loaded with DMAP-Au NPs have also been used as coatings on colloids, in order to modulate the optical response of colloidal crystals,[38-40] as electrochemical sensors,[34] or as nanostructured optically addressable capsules that can be irradiated with near-IR radiation for the controlled release of (bio)- macromolecules.[36, 37]

The ability to construct nanoparticle-based thin films with tailored properties, as well as their ultimate application, is dependent on a fundamental understanding of the interactions involved. In these condensed, organized films, the gold NPs displaying very different dielectric properties are subjected to strong interactions. These interactions between neighbouring gold particles generate collective plasmon resonances, controlled by the long-range aggregation of the gold NPs within the same layer.[41] A variable packing density and the corresponding interparticle distances, along with changes in the dielectric constant of the medium between particles are considered to be major factors affecting the dipolar-dipolar interactions and SPR frequency. Dipole-dipole interactions have been demonstrated to play a key role in optics of metal NPs, and especially in the case of closely spaced NP films, as has been recently shown by Ung et al.[21] for assemblies of silica-coated gold ($Au@SiO_2$) NPs on flat surfaces and by Caruso et al.[20] for assemblies on spheres. In these systems, the interparticle separation determines the plasmon oscillation frequency. Therefore, there is a substantial interest in the design of Au nanoparticulated films with control over the spacing between NPs, particularly in the distance range smaller than the NP diameter, where the optical and electronic properties change substantially with spacing. Furthermore such $Au@SiO_2$ NPs can be further functionalized through the reactivity of the hydroxide groups onto the silica surface, thereby facilitating chemical manipulation of the particle surfaces.

The early detection of structural damage in critical infrastructures is also a long-standing envisaged goal. In particular, a major limitation in the development of structural sensing systems is that they are incapable of detecting submicron-level damage due to their limited sensitivity at this scale. Following this goal, the use of photonic crystals in submicron damage detection has been recently proposed.[42] The idea arises from the use of the spectral response of photonic lattices, very sensitive to geometrical modifications, to reveal the strain in an adherent substrate through the induced microdamage on the photonic crystal structure. The application of such systems requires a precise fabrication of the photonic crystals which to date, has been demonstrated

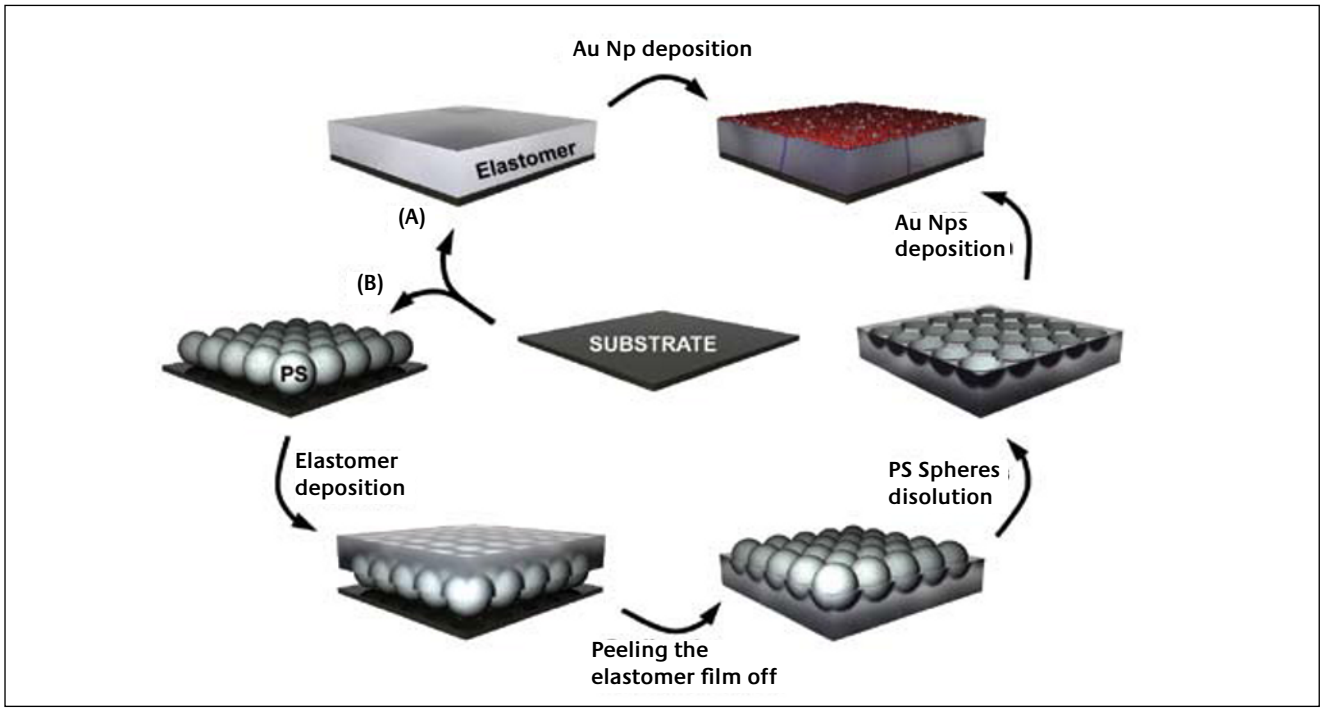


**Figure 1**

*Schematic illustration of the synthetic process followed for preparation of functionalized PDMS films. $Au@SiO_2$ NPs are deposited onto either planar PDMS elastomeric films (A), or on PDMS films with a close packed honeycomb-like hole structure (B).*

to be quite complicated to obtain with sufficient quality, over a variety of substrates and over large areas.

The interest of this manuscript resides in exploiting the optical properties of gold nanoparticulated films assembled onto elastomeric polydimethyl siloxane (PDMS) substrates, produced by the LbL self-assembly technique, for exploring their potential use in strain optical sensing applications. In general, composites made of gold NPs on organic thin films for optical sensing applications are based on a combination of NPs with suitable organic compounds, since this allows to control the chemical nature of the film material, and thereby the selectivity of the sensor device, while the physical properties of the NPs can be used for signal transduction. In this case however, the stretching dependent SPR intensity of a gold nanoparticulated film onto a polymeric PDMS substrate and a further refinement, based on using the same PDMS films, patterned with hexagonal close-packed ordered hole structure, as templates for the deposition of the $Au@SiO_2$ NPs is reported. Such dual functionalization provides strain sensing optical properties through both the intensity of the SPR and the modification of the diffraction pattern. A scheme, representative of the synthetic process, is illustrated in figure 1 and further detailed in the experimental section.

## Experimental

**PDMS polymeric films**. PDMS (polydimethyl siloxane; Sylgard 184 from Dow Corning GmbH ) elastomer films were obtained by deposition of a PDMS solution onto a silicon substrate, and onto a hexagonally close-packed ordered monolayer of polystyrene (PS) spheres. Both samples were dried at 60°C for 48 h to ensure a complete polymerization. The PDMS films were peeled off the silicon substrate in both cases, with the PS spheres partially embedded in the elastomeric film in the second case. The PS spheres can be completely embedded in the PDMS film through extensive (1 h) exposure of the film to vacuum prior to polymer curing. In order to obtain the close-packed honeycomb-like hole structure onto the PDMS elastomeric film, the PS spheres were dissolved by immersing the polymeric film in a chloroform solution for two hours.

**Hexagonally close-packed ordered arrays of PS spheres**. The hexagonally close-packed ordered arrays of PS spheres (2 x 5 $cm^2$) were prepared onto silicon substrates which were cleaned in a solution of 7% $NH_4OH$/30% $H_2O_2$/ water (1:1:5) for 60 min at 80°C, rinsed with milli-Q water, and dried under an argon stream. PS spheres (575 nm diameter, Microparticles gmbH, Berlin) were used as received (10% aqueous dispersion). The particle suspension was diluted by mixing with an equal volume of ethanol. The ethanol/water PS solution was slowly deposited on the surface of the pure water inside a 15 cm diameter Petri dish, using a glass pipette, so that a particle monolayer was formed. Part of the surface was not covered, in order to avoid the formation of cracks in the lattice during the following steps of the preparation. Finally, the monolayer was deposited on a substrate by slow water evaporation.

**Polyelectrolyte-coated substrates**. Polyelectrolyte-coated substrates (2 x 5 $cm^2$ PDMS film with an upper flat surface, and with a hexagonally close-packed ordered hole structure at the upper surface)[43] were prepared following the LbL self-assembly technique, which has been described elsewhere.[44] The same procedure was used in both cases: the PDMS substrate was first immersed in a solution of PDADMAC (polydiallyldimethylammonium chloride); Mw=400000-500000; 1wt. %, 0.5M NaCl) allowing polyelectrolyte adsorption over a period of 2 h. After rinsing the substrate several times with pure water, PSS (poly(sodium 4-styrenesulfonate); Mw=70000; 1mg $mL^{-1}$, 0.5 M NaCl) was deposited under the same conditions, followed by an additional layer of PDADMAC, which renders both surfaces positively charged.

**$Au@SiO_2$ NPs**. 25 nm silica-coated gold nanoparticles ($Au@SiO_2$) with a gold core of 15 nm and silica shell thickness of 6 nm (the synthesis process can be found elsewhere[45]) were deposited onto the polyelectrolyte-coated PDMS film by immersing the PDMS substrate in a solution of these negatively charged $Au@SiO_2$ NPs for 2 h. Excess $Au@SiO_2$ NPs were removed by rinsing the nanoparticulated film with pure water under mild sonication.

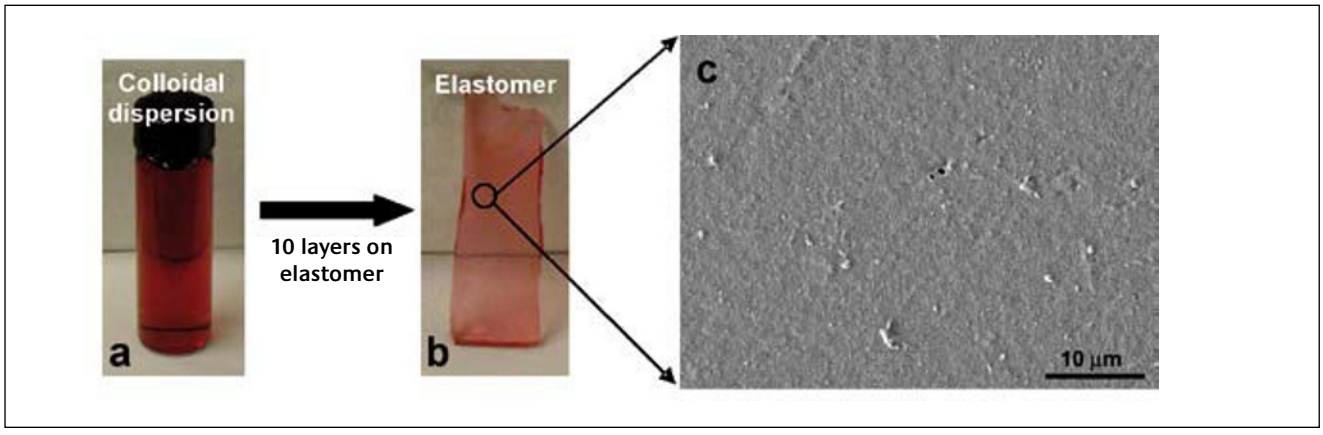


**Figure 2**

*Photographs of a typical colloidal solution of $Au@SiO_2$ NPs (a) and the sample obtained through assembly of 10 successive NP monolayers onto a flat PDMS film (b). (c) SEM image of the PDMS surface after deposition of the $Au@SiO_2$ NPs.*

**Polymer film stretching**. Samples of PDMS films with deposited Au@$SiO_2$ NPs , either flat or with a hexagonal close-packed ordered hole structure were stretched by the following experimental process. The film dimensions used were 50 mm long, 20 mm wide, and 3 mm thick. The samples were clamped and mounted onto an uniaxial loading frame inside an environmental chamber. The distance between clamps was 40 mm. A period of 10 min was allowed for the sample to reach the steady state temperature. The samples were uniaxially stretched at room temperature up to a total engineering strain of 3% at an average displacement rate of 0.5 mm/min. Both samples were stretched under the same conditions and, upon load removal, were allowed to relax back for a fixed period of time at the same temperature of the uniaxial test. The relaxation times varied up to a maximum of 2 h.

**Atomic Force Microscopy (AFM)**. AFM was used to obtain topographic images of the nanoparticle arrays. The images were taken in ambient conditions with a Veeco DI 3100 microscope with a Nanoscope IIIa controller operating in tapping mode.

**UV-vis spectroscopy**. UV-vis spectra were collected using a Shimadzu UV-3101 PC UV-visible spectrometer over the range 200-1100nm. The gold nanoparticulated films onto polymeric substrates were incorporated to the sample holder by gluing.

## Results and Discussion

It is well known that using Au@$SiO_2$ NPs of various shell thickness, homogeneous films can be assembled onto different substrates (e.g. glass or PS spheres), with tunable optical properties. Depending on the silica shell thickness, it is possible to determine the spacing between neighbouring particles and in turn to tailor their dipolar coupling.[20] Since gold nanoparticles themselves have strongly size dependent optical properties, the optical response measured from films can be due to both the intrinsic particle size effects and to the controlled distance between neighbouring gold particles. 15 nm Au NPs with homogeneous size distribution and further coated with a 6 nm thick silica shells were therefore selected for the proposed sensing application, taking into account that the silica shells in such films will screen the gold interparticle interactions onto substrates, thus leading to a much sharper SPR band detected by UV-vis spectroscopy.

Figure 2 (a,b) illustrates the appearance of a sample of Au@$SiO_2$ NPs in solution (a) and the elastomeric PDMS film coated with the same core-shell NPs (b). From the photographs one can see that the colour is retained once the NPs are deposited onto the polymeric film. The colour appears uniform over the whole sample, revealing a homogeneous deposition of Au@$SiO_2$ NPs onto the PDMS surface. This homogeneous coating of the elastomer was confirmed through measurement of UV-vis spectra along the film, which yielded similar absorbance intensity, and is also illustrated on the SEM image of figure 2c.

While after a stretching procedure of this PDMS-Au NPs film a gradual decrease of intensity was observed in the UV-vis absorbance spectra, the opposite trend was registered when the film was compressed (figure 3a). A linear dependence of absorbance (measured at the wavelength of the maximum of the gold plasmon band) against stretching or compressing is also plotted (inset figure 3a), illustrating the easy and quick monitoring of the strain the film is undergoing. It is also important to underline the sensitivity of the method, taking into account that these experiments have been recorded using a standard UV-vis spectrophotometer with a beam diameter over the sample of 0.5 cm.

In principle one may expect two different effects to arise from the stretching experiments, both of them responsible for the subsequent optical response. One can anticipate on one hand that all neighbouring Au@$SiO_2$ NPs will just separate homogeneously from each other to an average distance proportional to the stretching intensity (figure 3b, I). However, on the other hand, one can also foresee the formation of localized cracks on the surface due to the same stretching process. Debonding of few neighbouring particles as their

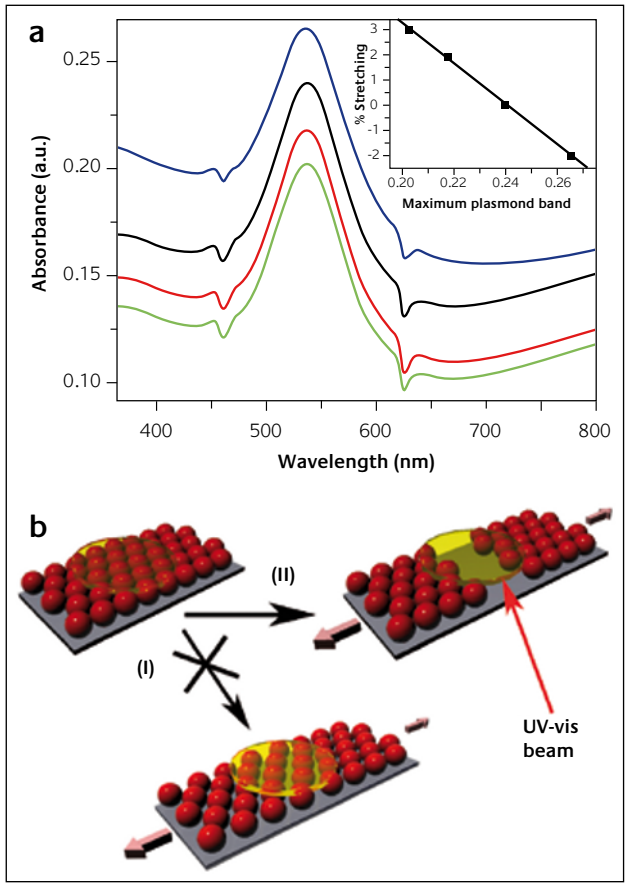


**Figure 3**

*a) UV-vis spectra of a Au@$SiO_2$ nanoparticle layer deposited onto PDMS film. Spectra correspond to sample as prepared (black line); after stretching (2%) (red line) and (3%) (green line); after compression (2%) (blue line) (Inset: linear dependence behaviour). b) Representative scheme of the stretched film assuming the formation of cracks (I), and the uniform separation between the particles (II).*

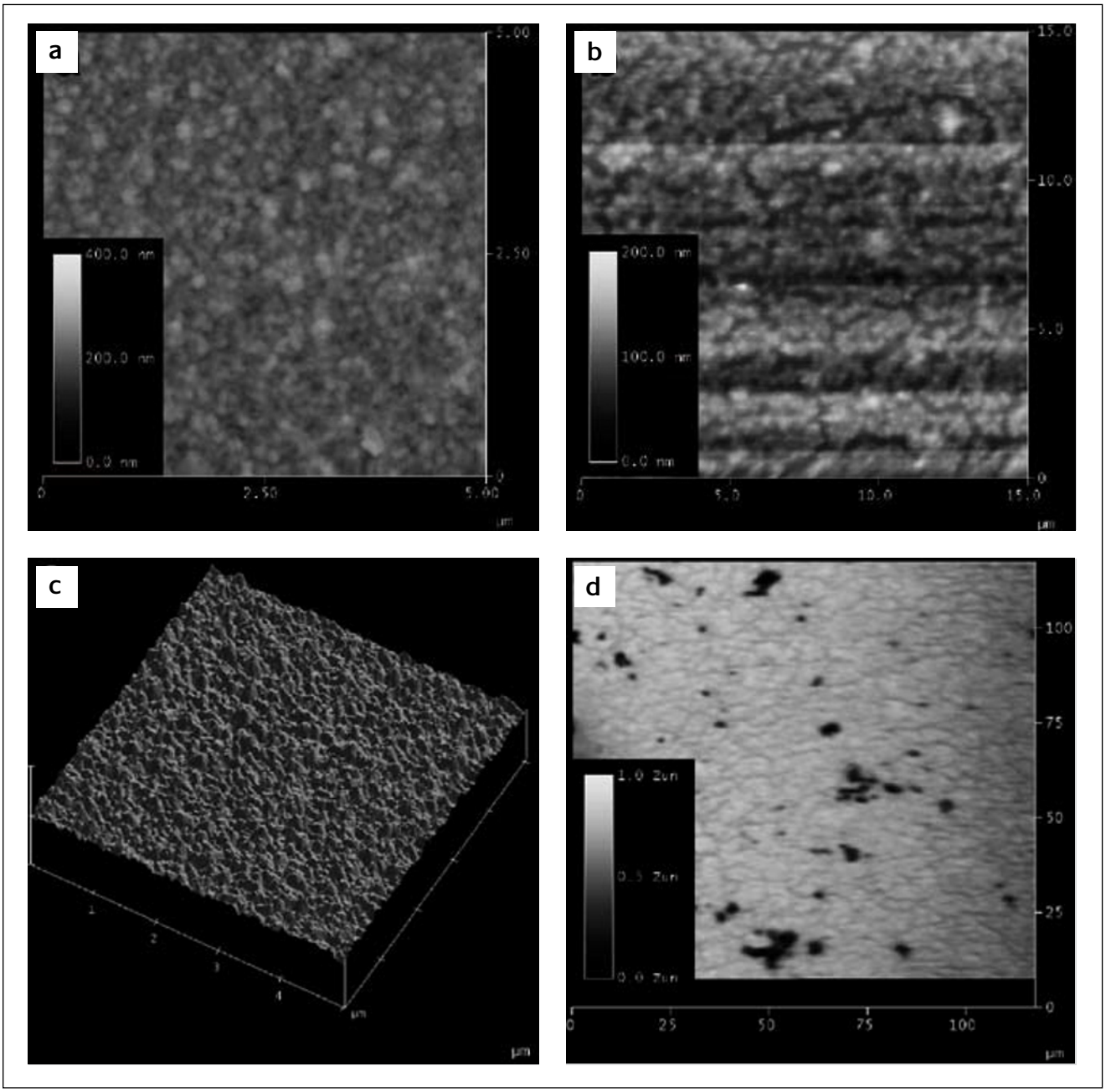


**Figure 4**

*AFM images of the nanoparticulated film onto the PDMS elastomer before (a, c) and after the stretching process (b, d).*

separation increases may produce a domino effect leading to propagation of nucleated defects and to the formation of extended close packed groups of these NPs (figure 3b, II). In the first hypothesis, the NPs would separate from each other with no cracks forming on the surface. This would be very convenient if gold NPs with short capping agents rather than the outer silica shell were used, ensuring a short separation distance and the corresponding strong dipolar interactions resulting in a red shift of the SPR in the UV-vis spectra. In that case, the applied stretching would lead to increased average separation between neighbouring gold NPs which would be monitored as a gradual blue shift of the gold SPR in the UV-vis spectra until reaching enough distance to avoid the dipolar interactions (typically of the order of one particle diameter).[20] If this first hypothesis were right, these measurements could be used for microdamage detection systems attending to the position of the maximum of the gold plasmon band in the UV-vis spectra.

The second hypothesis sustains a random formation of localized cracks in the nanoparticulated coating acting as spacers between groups of NPs, in such a way that individual particles will not be separated but rather form big agglomerates. The formation of these cracks in the nanoparticulated film would therefore not avoid the dipolar interactions, and the expected blue shift of the SPR maximum would not be observed. Under these conditions, we would not obtain information over the stretching behaviour of the film if only the SPR position was considered. However, the formation of these cracks in the nanoparticulated film upon stretching of the PDMS elastomeric film would decrease the amount of

gold NPs illuminated by the UV-vis beam, thereby lowering the absorbance intensity of the gold SPR, proportionally to the stretching force.

Conversely to the tensile case, when the film is compressed the amount of particles under the beam increases and so does the absorbance. Cracking is more difficult though it can still happen at higher stress levels by means of shear banding or splitting, which are active damage mechanisms in compressions[46].

With the purpose of inspecting the morphology of the coated elastomeric film, to elucidate which of the suggested paths has been followed and therefore to understand the optical behaviour of the deposited gold films onto the PDMS elastomeric substrates upon stretching, these nanoparticulated films were investigated by atomic force microscopy (AFM). Initially, after LbL deposition of 10 layers of $Au@SiO_2$ NPs onto the PDMS elastomer, the as prepared film appeared homogeneous, with no sign of cracks (figure 4a). However, when the substrate was stretched some particles became separated, forming evident cracks on the surface of the film (figure 4b and d), thus justifying the second hypothesis with formation of agglomerates rather than a homogeneous separation of NPs.

The presence of these cracks in the nanoparticulated film together with no shift in the UV-vis spectra, justify the use of $Au@SiO_2$ NPs. The 5 nm thickness of the silica shell of $Au@SiO_2$ NPs ensures a distance of (at least) 10 nm between the gold cores, which is sufficient in this case to avoid interparticle coupling interactions and therefore to maintain a sharp SPR band. The absence of silica spacer between gold NPs would result in interparticle plasmon coupling, which would be reflected into a much broader and red-shifted SPR band.

The results demonstrate that the $Au@SiO_2$ NPs coating film is potentially sensitive to the strain field anomalies typically associated with the presence of defects in the underlying substrate and can reveal ongoing damage formation in the submicron scale.

A further refinement of the procedure comprises the use of a hexagonal close packed monolayer of PS spheres as a mask to shape the PDMS polymer. The polymeric PS spheres monolayer can be partially (figure 5a) or totally embedded (figure 5b) in the PDMS elastomer, and the spheres can be further dissolved (figure 5c and d) (details in the experimental section). It is interesting to note, taking into consideration the SEM images in figure 5, the different morphology of the PDMS film after removing the PS particles, depending on the partial or total embedding of the PS spheres, though the diffraction pattern of the structures was preserved.

The PDMS elastomeric film sample with such a structured surface morphology, as shown in the SEM image of figure

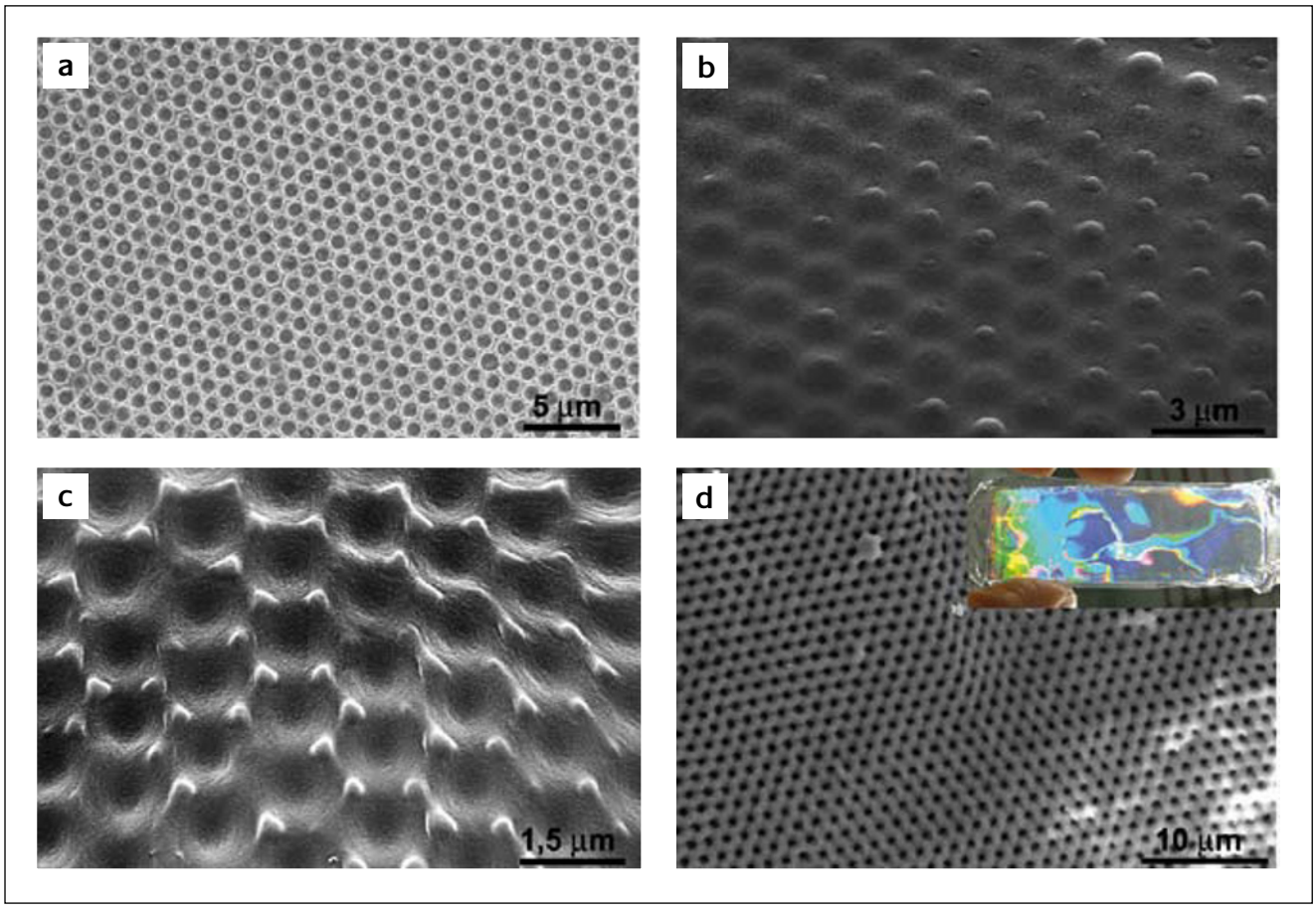


**Figure 5**

*SEM images of the hexagonal close packed monolayers of PS spheres partially (a) and almost totally embedded in the PDMS elastomer (b); and after dissolution of the PS spheres in the respective samples (c, d). Inset: photograph of the PDMS film (2x5 $cm^2$) with an ordered structure of holes.*

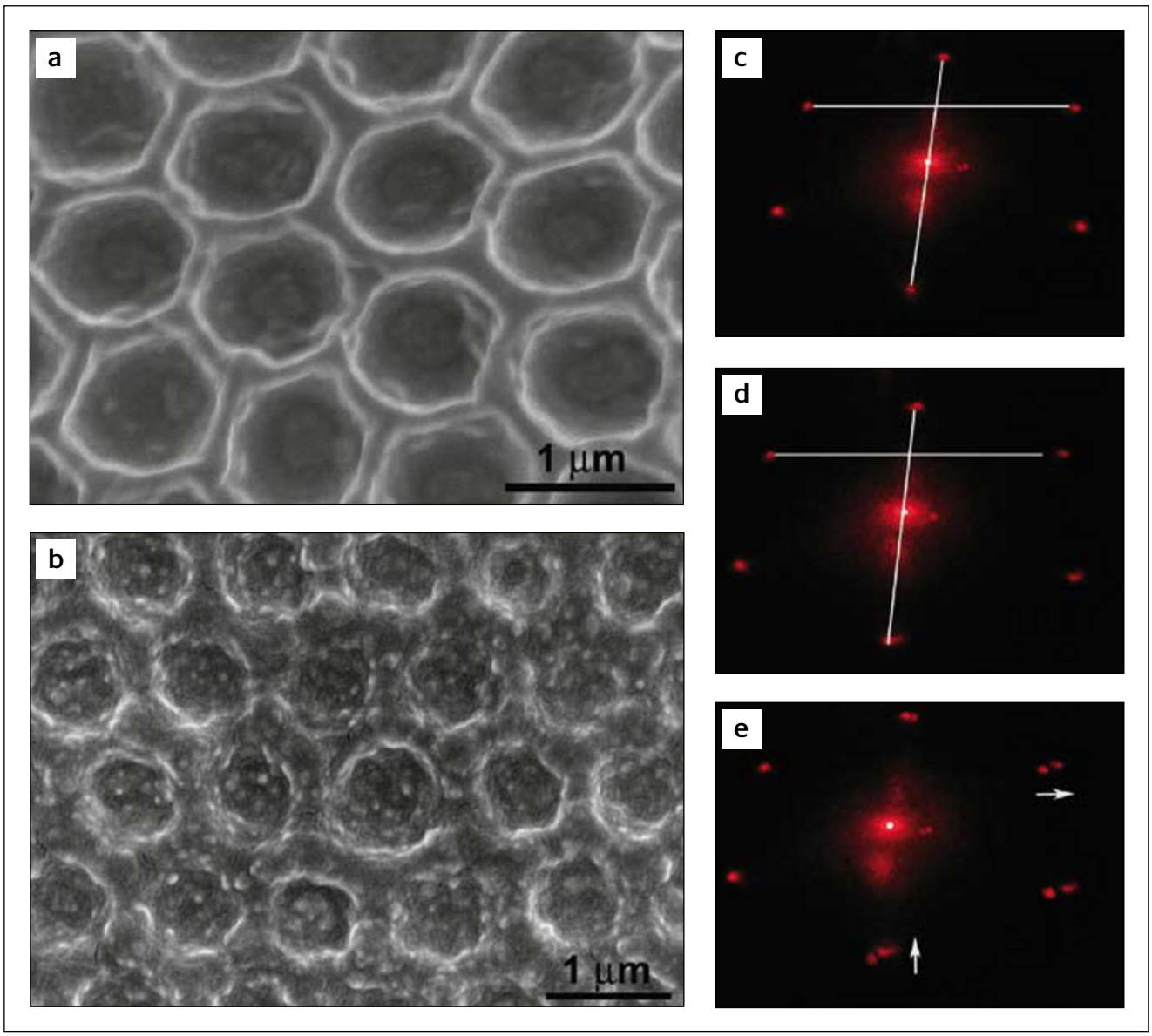


**Figure 6**

*SEM images of the PDMS elastomeric films surface with an ordered structure of holes before (a) and after deposition of 10 monolayers of Au@$SiO_2$ NPs (b). Diffraction pattern of the composite PDMS-gold film before (c) and after (d) the stretching process, and their superposition (e).*

5c, shows intense reflected colors due to the ordered hole structure of the PDMS surface (inset of figure 5d). Moreover, when a laser beam is irradiated from the top, perpendicular to the sample plane and traversing it, a perfect hexagonal diffraction pattern arising from the honeycomb hole structure in the PDMS surface can be clearly observed (figure 6b). This second behaviour of the polymer film due to the ordered structure could also be utilized for strain sensing applications, since when the patterned elastomer is stretched, the holes become deformed and this modification is reflected in the diffraction pattern.

We have used the patterned elastomer film as a substrate, with the ordered structure of holes in their surface (which offers a higher surface area for NPs deposition than the corresponding flat surface) for the deposition of a nanoparticulated film composed of 10 monolayers of Au@$SiO_2$ NPs. The SEM images in figure 6 show the PDMS substrate before (figure 6a, illustrating the initial hole-based structure) and after the deposition of the 10 monolayers of Au@$SiO_2$ NPs (figure 6b). It is interesting to note that the nanoparticulated gold/silica film does not screen the hexagonal diffraction pattern, in such a way that both physical phenomena, diffraction and SPR, can be simultaneously exploited for optical sensing. Identical UV-vis absorbance changes (data not shown) were observed as in the case of the flat elastomeric substrate, with the stretching process driving the agglomeration of Au@$SiO_2$ NPs in separate groups due to the formation of cracks in the film.

## Conclusions

In summary, we have discussed the use of dense Au@SiO2 NPs films built up by means of the LbL method onto PDMS elastomeric films, for optical sensing applications. We have compared the responses of planar and hexagonal

close-packed ordered holes structure patterned thin films of PDMS polymeric substrates. The Au@SiO2 NPs SPR intensity and the diffraction pattern owed to the ordered structure onto the polymer surface, preserved after the NPs deposition and the stretching process, become independent physical phenomena which are active for optical strain detection.

## Acknowledgements

M. A. C.-D. and V. S.-M. acknowledge the financial support from the *Isidro Parga Pondal* Program (Xunta de Galicia, Spain). This work has been partially supported by the Spanish Xunta de Galicia under grant No. PGIDIT03TMT30101PR and by AFOSR.

## About the Author

**Miguel A. Correa-Duarte** obtained a PhD degree in Chemistry from the University of Vigo in 2002 and since then had postdoctoral position in CAESAR (Bonn) and a visiting research assistant professor position in Arizona State University (USA). He currently holds an associate researcher position at the Department of Physical Chemistry at the University of Vigo. His research interest is in the field of Nanoscience and Nanotechnology, including carbon nanotube functionalization and carbon nanotube-based hybrid materials, core-shell nanoparticles and composites. He has previously worked in business for chemistry-related companies.

## References

1 N. Krasteva, I. Besnard, B. Guse, R. E. Bauer, K. Muellen, A. Yasuda, T. Vossmeyer, *Nano Letters* **2002**, *2*, 551
2 G. Raschke, S. Kowarik, T. Franzl, C. Soennichsen, T. A. Klar, J. Feldmann, A. Nichtl, K. Kuerzinger, *Nano Letters* **2003**, *3*, 935
3 Y. Cao, R. Jin, C. A. Mirkin, *Journal of the American Chemical Society* **2001**, *123*, 7961
4 J. H. Fendler, *Chemistry of Materials* **2001**, *13*, 3196
5 C. A. Mirkin, *Inorganic Chemistry* **2000**, *39*, 2258
6 T. Morris, H. Copeland, E. McLinden, S. Wilson, G. Szulczewski, *Langmuir* **2002**, *18*, 7261
7 N. Nath, A. Chilkoti, *Journal of the American Chemical Society* **2001**, *123*, 8197
8 S. R. Sershen, S. L. Westcott, N. J. Halas, J. L. West, *Applied Physics Letters* **2002**, *80*, 4609
9 Z.-S. Wang, T. Sasaki, M. Muramatsu, Y. Ebina, T. Tanaka, L. Wang, M. Watanabe, *Chemistry of Materials* **2003**, *15*, 807
10 A. Henglein, *Journal of Physical Chemistry* **1993**, *97*, 5457
11 P. Mulvaney, *Langmuir* **1996**, *12*, 788
12 S. Link, M. A. El-Sayed, *Journal of Physical Chemistry B* **1999**, *103*, 8410
13 S. J. Oldenburg, R. D. Averitt, S. L. Westcott, N. J. Halas, *Chemical Physics Letters* **1998**, *288*, 243
14 L. M. Liz-Marzán, *Langmuir* **2006**, *22*, 32
15 C. Y. Chen, E. Burstein, *Physical Review Letters* **1980**, *45*, 1287
16 S. Link, M. A. El-Sayed, *Journal of Physical Chemistry B* **1999**, *103*, 4212
17 T. Teranishi, S. Hasegawa, T. Shimizu, M. Miyake, *Advanced Materials (Weinheim, Germany)* **2001**, *13*, 1699
18 S. Link, C. Burda, M. B. Mohamed, B. Nikoobakht, M. A. El-Sayed, *Journal of Physical Chemistry A* **1999**, *103*, 1165
19 C. P. Collier, R. J. Saykally, J. J. Shiang, S. E. Henrichs, J. R. Heath, *Science (Washington, D. C.)* **1997**, *277*, 1978
20 F. Caruso, M. Spasova, V. Salgueirino-Maceira, L. M. Liz-Marzán, *Advanced Materials (Weinheim, Germany)* **2001**, *13*, 1090
21 T. Ung, L. M. Liz-Marzán, P. Mulvaney, *Journal of Physical Chemistry B* **2001**, *105*, 3441
22 J. Schmitt, P. Maechtle, D. Eck, H. Moehwald, C. A. Helm, *Langmuir* **1999**, *15*, **3256**
23 H. Fan, K. Yang, D. M. Boye, T. Sigmon, K. J. Malloy, H. Xu, G. P. Lopez, C. J. Brinker, *Science (Washington, DC, United States)* **2004**, *304*, 567
24 M. P. Rowe, K. E. Plass, K. Kim, C. Kurdak, E. T. Zellers, A. J. Matzger, *Chemistry of Materials* **2004**, *16*, 3513
25 M. Brust, D. Bethell, D. J. Schiffrin, C. J. Kiely, *Advanced Materials (Weinheim, Germany)* **1995**, *7*, 795
26 N. Fishelson, I. Shkrob, O. Lev, J. Gun, A. D. Modestov, *Langmuir* **2001**, *17*, 403
27 J. Y. Tseng, M. H. Lin, L. K. Chau, *Colloids and Surfaces, A: Physicochemical and Engineering Aspects* **2001**, 1*82*, 239
28 R. G. Freeman, K. C. Grabar, K. J. Allison, R. M. Bright, J. A. Davis, A. P. Guthrie, M. B. Hommer, M. A. Jackson, P. C. Smith, et al., *Science (Washington, D. C.)* **1995**, *267*, 1629
29 K. C. Grabar, R. G. Freeman, M. B. Hommer, M. J. Natan, *Analytical Chemistry* **1995**, *67*, 735
30 A. N. Shipway, M. Lahav, I. Willner, *Advanced Materials (Weinheim, Germany)* **2000**, *12*, 993
31 D. L. Feldheim, K. C. Grabar, M. J. Natan, T. E. Mallouk, *Journal of the American Chemical Society* **1996**, *118*, 7640
32 R. K. Iler, J. Colloid, *Interface Sci.* **1966,** *21*, 569
33 J. Schmitt, G. Decher, W. J. Dressick, S. L. Brandow, R. E. Geer, R. Shashidhar, J. M. Calvert, *Advanced Materials (Weinheim, Germany)* **1997**, *9*, 61
34 A. Yu, Z. Liang, J. Cho, F. Caruso, *Nano Letters* **2003**, *3*, 1203
35 D. I. Gittins, A. S. Susha, B. Schoeler, F. Caruso, *Adv. Mater.* **2002**, *14*, 508
36 A. S. Angelatos, B. Radt, F. Caruso, *Journal of Physical Chemistry B* **2005**, *109*, 3071
37 B. Radt, T. A. Smith, F. Caruso, *Advanced Materials (Weinheim, Germany)* **2004**, *16*, 2184
38 P. T. Miclea, A. S. Susha, Z. Liang, F. Caruso, C. M. Sotomayor Torres, S. G. Romanov, *Applied Physics Letters* **2004**, *84*, 3960
39 Z. Liang, A. Susha, F. Caruso, *Chemistry of Materials* **2003**, *15*, 3176

40 Z. Liang, A. S. Susha, F. Caruso, *Advanced Materials (Weinheim, Germany)* **2002**, *14*, 1160
41 W. Rechberger, A. Hohenau, A. Leitner, J. R. Krenn, B. Lamprecht, F. R. Aussenegg, *Optics Communications* **2003**, *220*, 137
42 I. El-Kady, M. M. R. Taha, M. F. Su, *Applied Physics Letters* **2006**, *88*, 253109
43 A. Kosiorek, W. Kandulski, P. Chudzinski, K. Kempa, M. Giersig, *Nano Lett*. **2004**, *4*, 1359
44 M. A. Correa-Duarte, M. Giersig, N. A. Kotov, L. M. Liz-Marzán, *Langmuir* **1998**, *14*, 6430
45 L. M. Liz-Marzán, M. Giersig, P. Mulvaney, *Langmuir* **1996**, *12*, 4329
46 Krajcinovic D., *Damage Mechanics, North-Holland Series in Applied Mathematics and Mechanics* **1996**, Vol. 41, Elsevier, Amsterdam